SI Appendix

RNA-protein interaction mapping via MS2 or Cas13-based APEX targeting

Shuo Han[a,b,c,1], Boxuan Simen Zhao[a,b,c,1], Samuel A. Myers[d], Steven A. Carr[d], Chuan He[e,f] and Alice Y. Ting[a,b,c,2]

[a]Department of Genetics, Chan Zuckerberg Biohub, Stanford University, Stanford, CA 94305;

[b]Department of Biology, Chan Zuckerberg Biohub, Stanford University, Stanford, CA 94305;

[c]Department of Chemistry, Chan Zuckerberg Biohub, Stanford University, Stanford, CA 94305;

[d]The Broad Institute of MIT and Harvard, Cambridge, MA 02142;

[e]Department of Chemistry, Institute for Biophysical Dynamics, Howard Hughes Medical Institute, University of Chicago, Chicago, IL 60637;

[f]Department of Biochemistry and Molecular Biology, Institute for Biophysical Dynamics, Howard Hughes Medical Institute, University of Chicago, Chicago, IL 60637;

[1]These authors contributed equally to this work.

[2]To whom correspondence may be addressed. Email: ayting@stanford.edu.

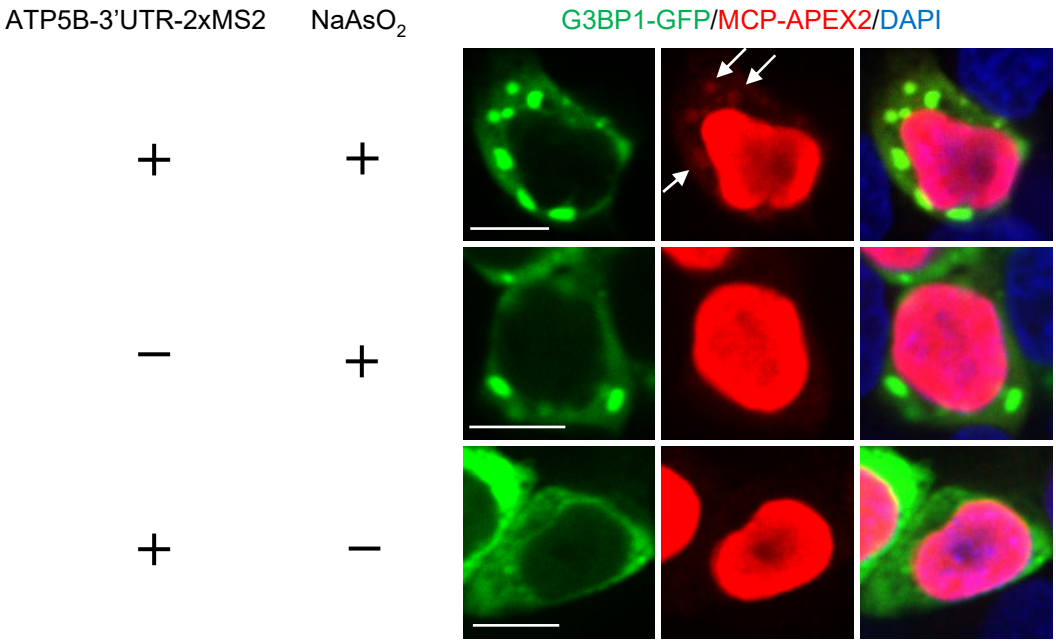

Figure S1. Fluorescence imaging of MCP-APEX2 binding to ATP5B mRNA during stress granule formation. HEK293T cells are transfected with ATP5B-3'UTR-2xMS2 and treated with $NaAsO_2$ for 30 minutes to induce stress granule formation. MCP-APEX2 is visualized by anti-V5 staining (Alexa Fluor 647, red). Stress granules are visualized with G3BP1-GFP (green). The nucleus is stained with DAPI. White arrows show co-localization of stress granules and MCP-APEX2 only in the presence of both ATP5B-3'UTR-2xMS2 and $NaAsO_2$ treatment. Scale bar, 10 μm.

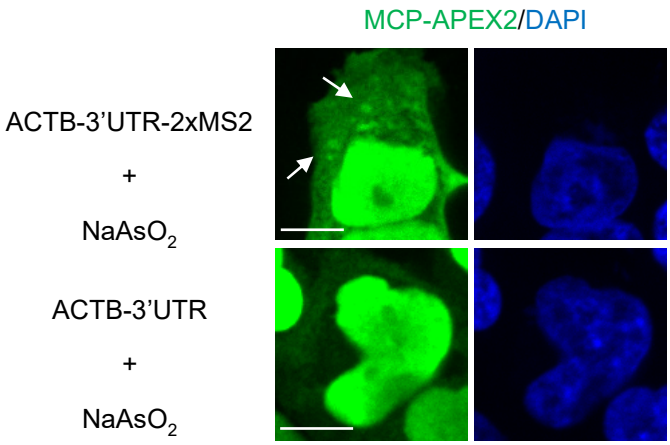

Figure S2. Fluorescence imaging of MCP-APEX2 binding to ACTB mRNA during stress granule formation. HEK293T cells are transfected with ACTB-3'UTR-2xMS2 and treated with $NaAsO_2$ for 30 minutes to induce stress granule formation. MCP-APEX2 is visualized by anti-V5 staining (Alexa Fluor 488, green). The nucleus is stained with DAPI. White arrows show the granule structures formed by MCP-APEX2 in the presence of ACTB-3'UTR-2xMS2 and $NaAsO_2$ treatment, but not in the untagged ACTB-3'UTR control. Scale bar, 10 μm.

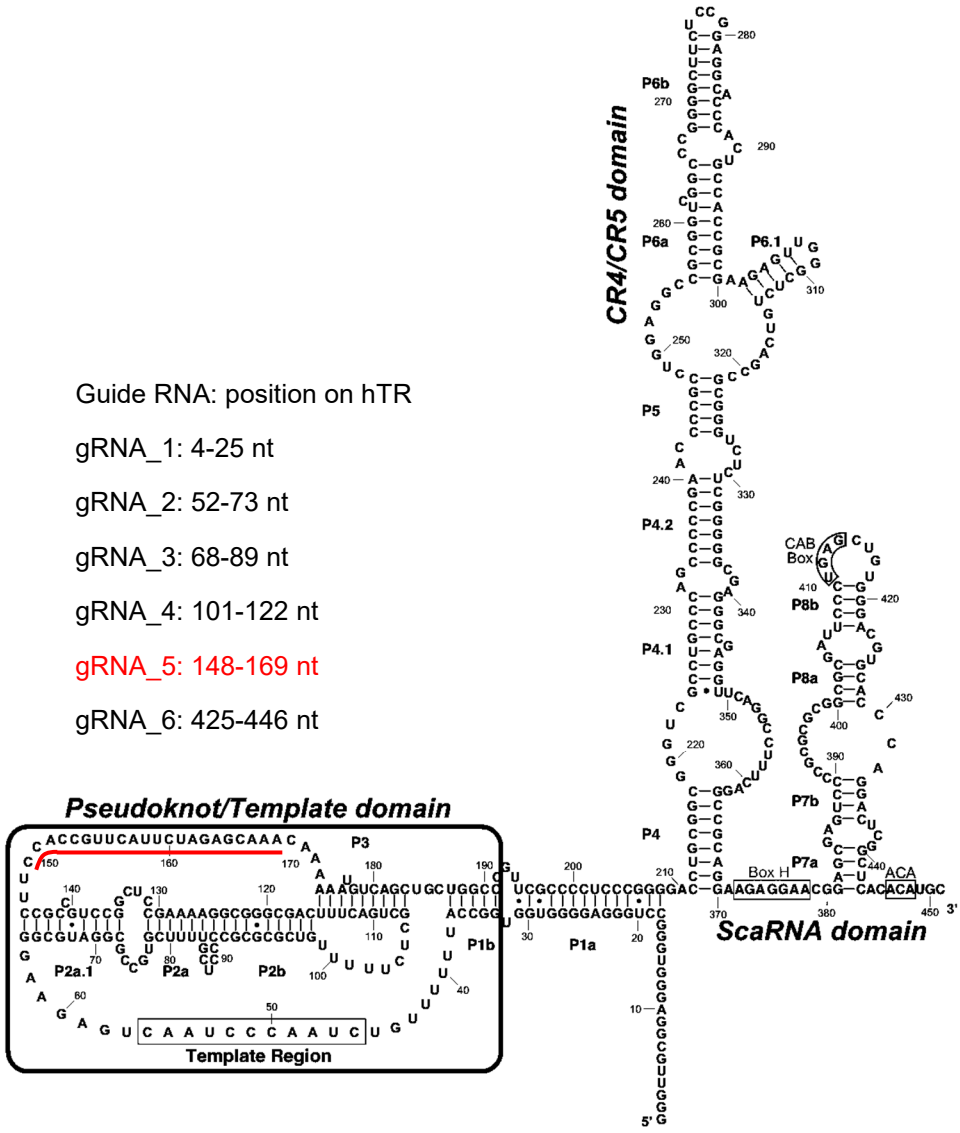

Figure S3. Sequence and structure of the human telomerase RNA. The spacer sequences of the RfxCas13d guide RNAs that showed significant knockdown are listed according to their position on hTR. gRNA_5 and its targeting region are highlighted in red. The structure of hTR is adapted from (1) and http://telomerase.asu.edu/structures.html.

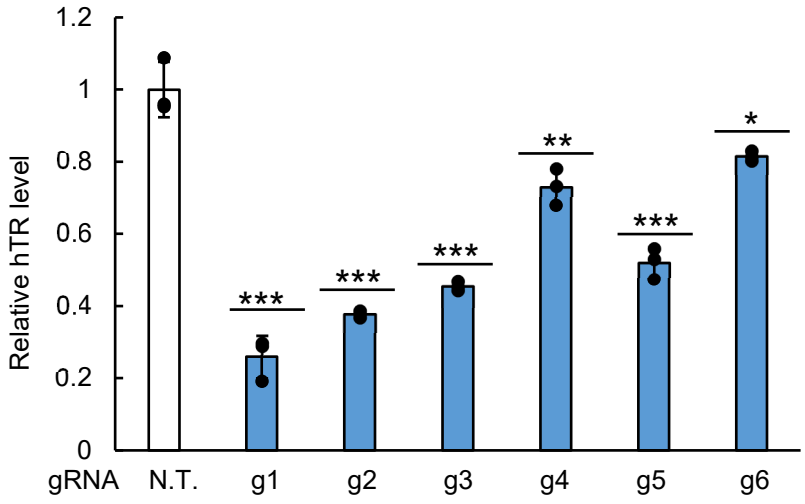

Figure S4. Testing hTR gRNA by knockdown with RfxCas13d. HEK 293T cells were co-transfected with RfxCas13d and the indicated gRNA. The expression level of hTR was quantified by RT-qPCR following total RNA extraction and normalized against the nontargeting (NT) gRNA control. Data are analyzed using a one-tailed Student's t-test (n=3). *, $p<0.05$; **, $p<0.005$; ***, $p<0.0005$.

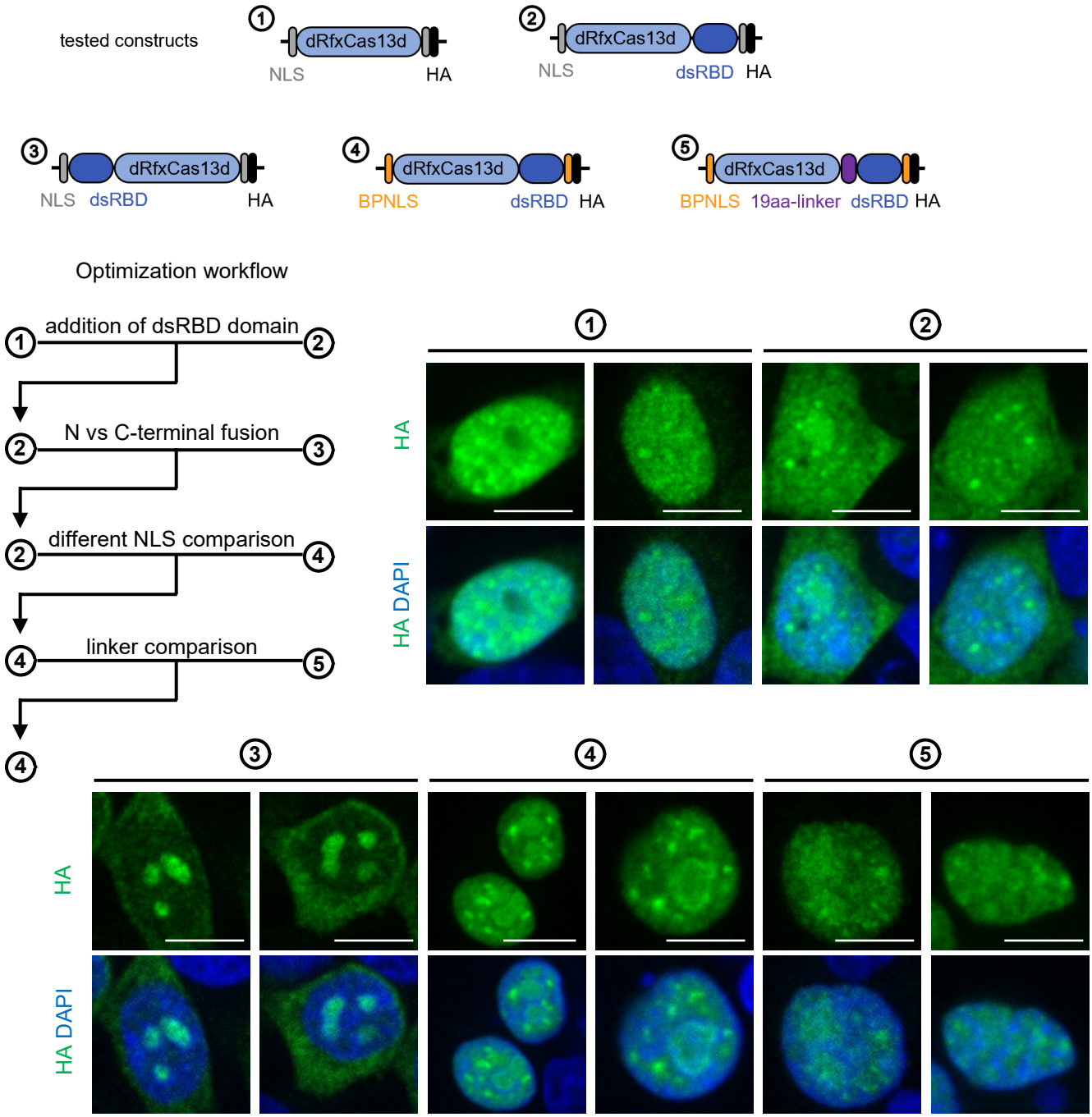

Figure S5. dCas13d-dsRBD optimization process. The addition of dsRBD domain to the C-terminus of dRfxCas13d improves the targeting to hTR foci: ② is better than ①. Compared to C-terminal dsRBD fusion, fusing dsRBD to the N-terminus of dRfxCas13d results in nucleolar aggregates: ② is better than ③. Replacing SV40 NLS with BPNLS improves dCas13d-dsRBD localization into the nucleus: ④ is better than ②. The addition of a flexible 19-amino acid glycine-serine linker between dCas13d and dsRBD diminishes the improved targeting: ④ is better than ⑤. All constructs are tested by co-transfection with hTR and hTR targeting gRNA in HEK293T cells. dRfxCas13d is visualized by anti-HA staining (Alexa Fluor 488, green). The nucleus is stained with DAPI (blue). Scale bars, 10 μm.

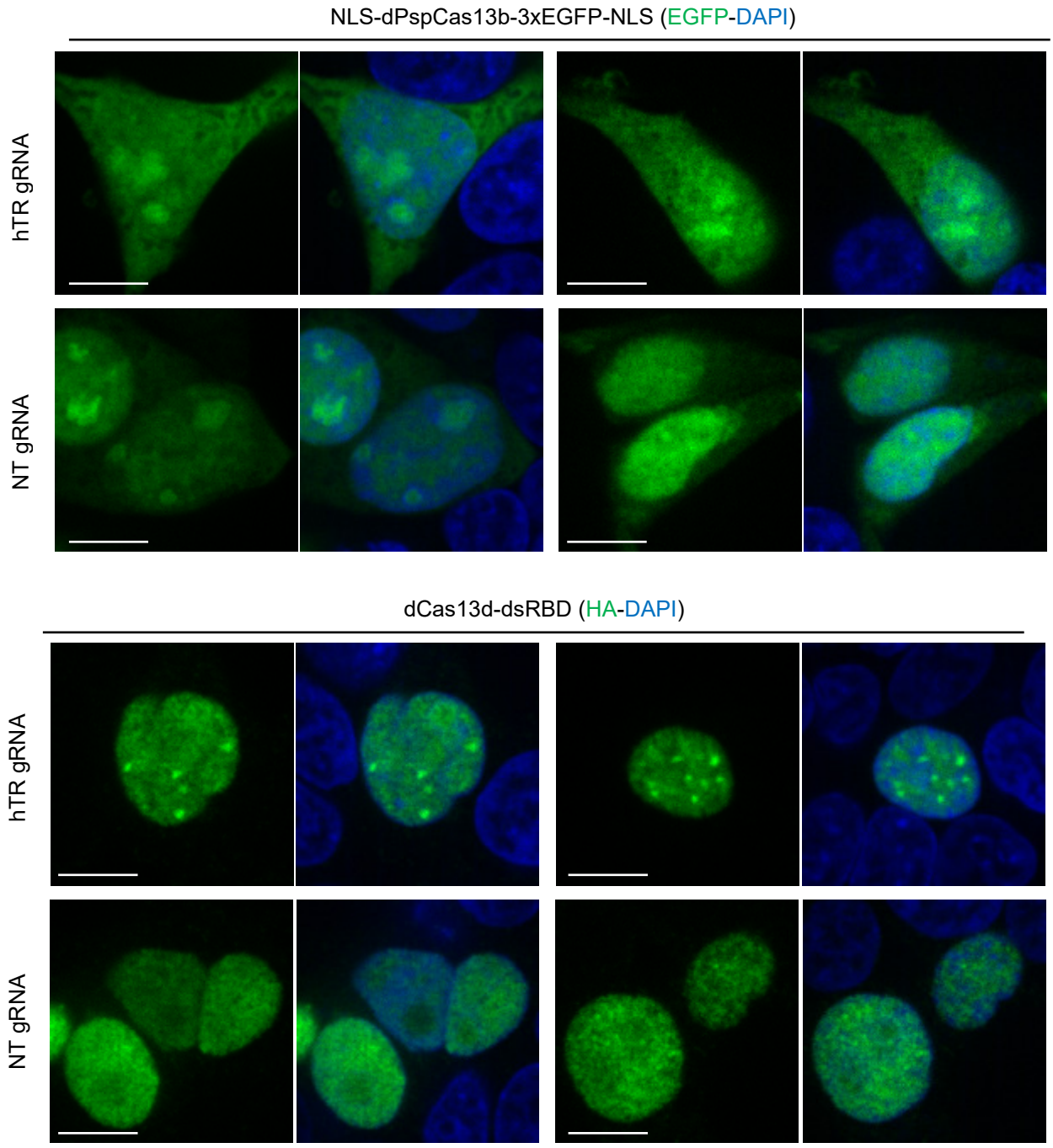

Figure S6. Fluorescence imaging of dPspCas13b (2) and dCas13d-dsRBD localization to hTR. HEK293T cells were transfected with hTR, either NLS-dPspCas13b-3xEGFP-NLS or dCas13d-dsRBD, and position-matched guide RNAs. The cells were then fixed and directly imaged by EGFP (top, green) or stained with anti-HA antibody (bottom, Alexa Fluor 488, green) to visualize the Cas13 protein and DAPI (blue, nuclei). Scale bars, 10 μm.

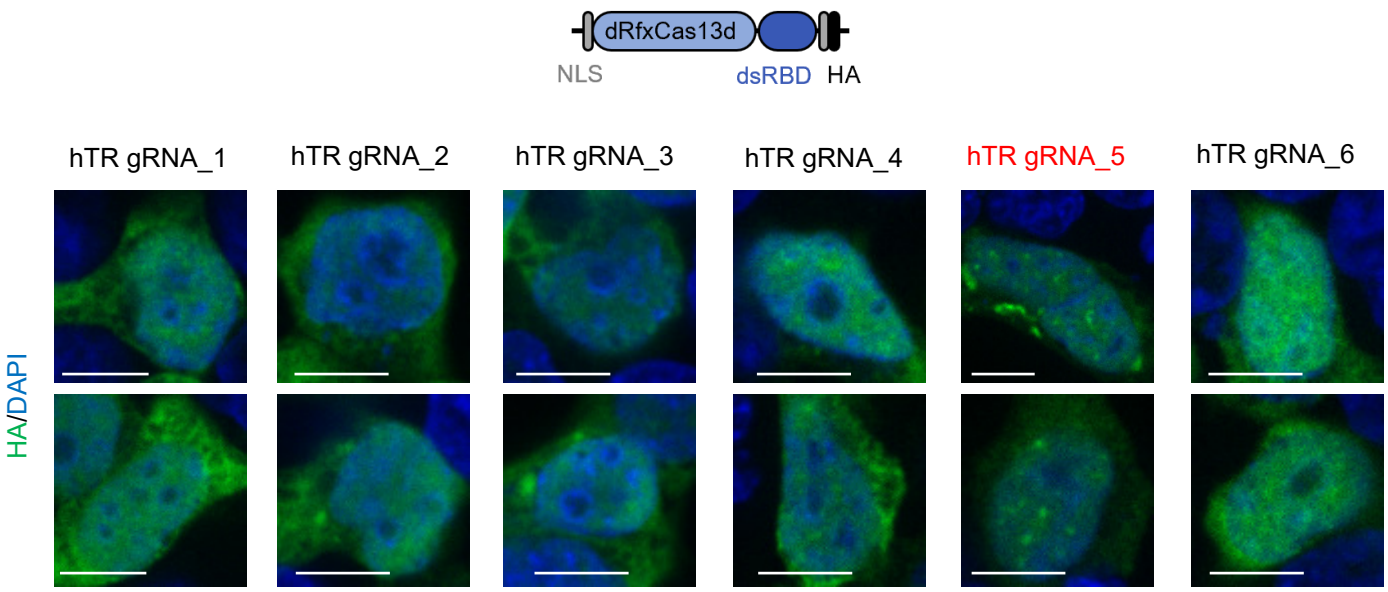

Figure S7. Testing hTR gRNA by fluorescence imaging. The indicated hTR gRNA was tested by co-transfection with hTR and NLS-dRfxCas13d-dsRBD in HEK293T cells. dRfxCas13d is visualized by anti-HA staining (Alexa Fluor 488, green). The nucleus is stained with DAPI (blue). Two fields of view are shown for each gRNA. hTR gRNA_5 is highlighted in red. Scale bars, 10 μm.

dRfxCas13d + hTR gRNA

HA-DAPI-hTR(3xFLAG-hTERT)

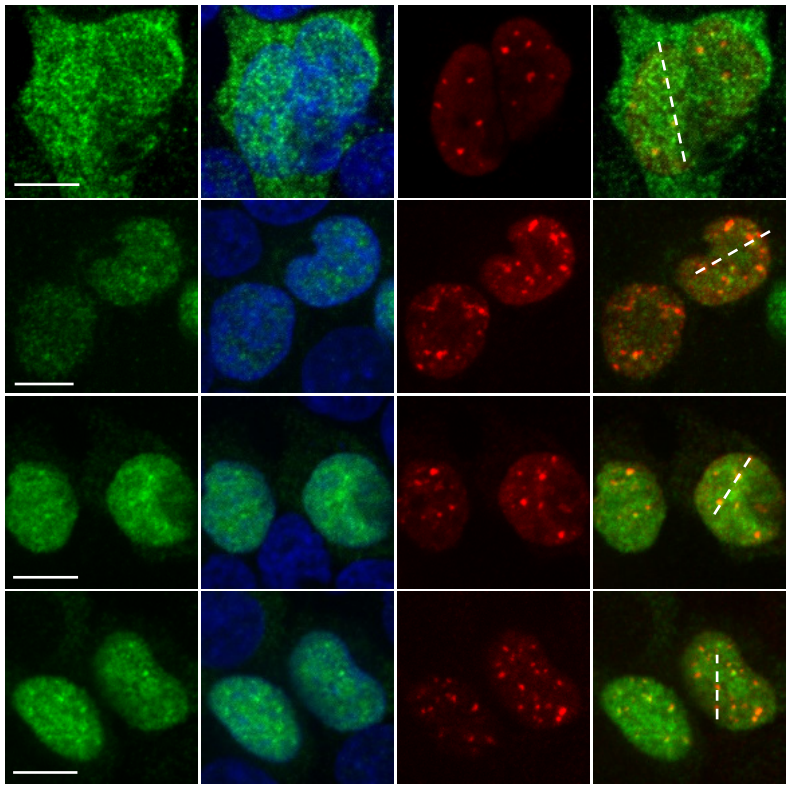

relative intensity

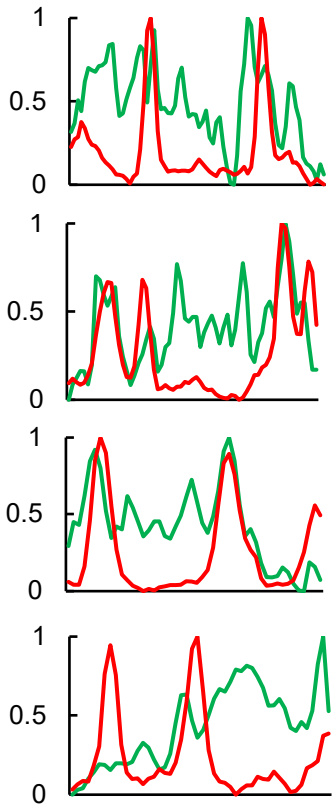

dRfxCas13d + NT gRNA

HA-DAPI-hTR(3xFLAG-hTERT)

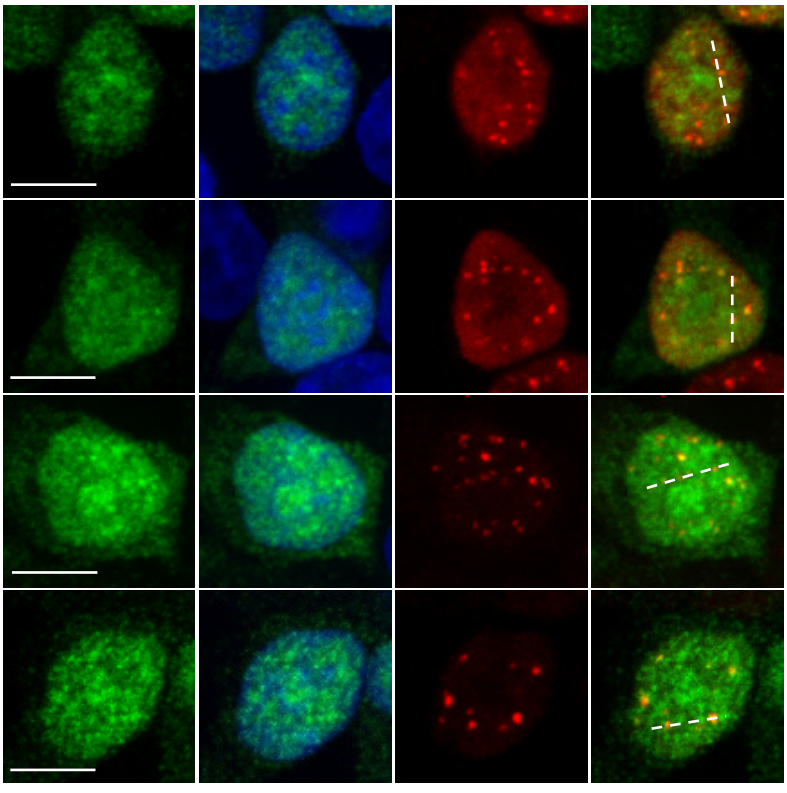

relative intensity

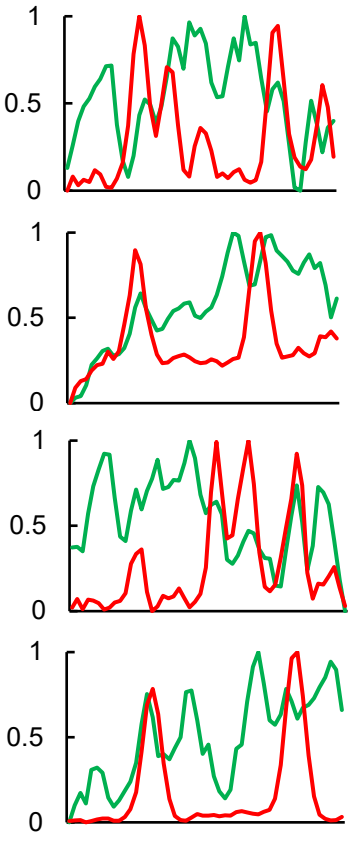

dCas13d-dsRBD + hTR gRNA

HA-DAPI-hTR(3xFLAG-hTERT)

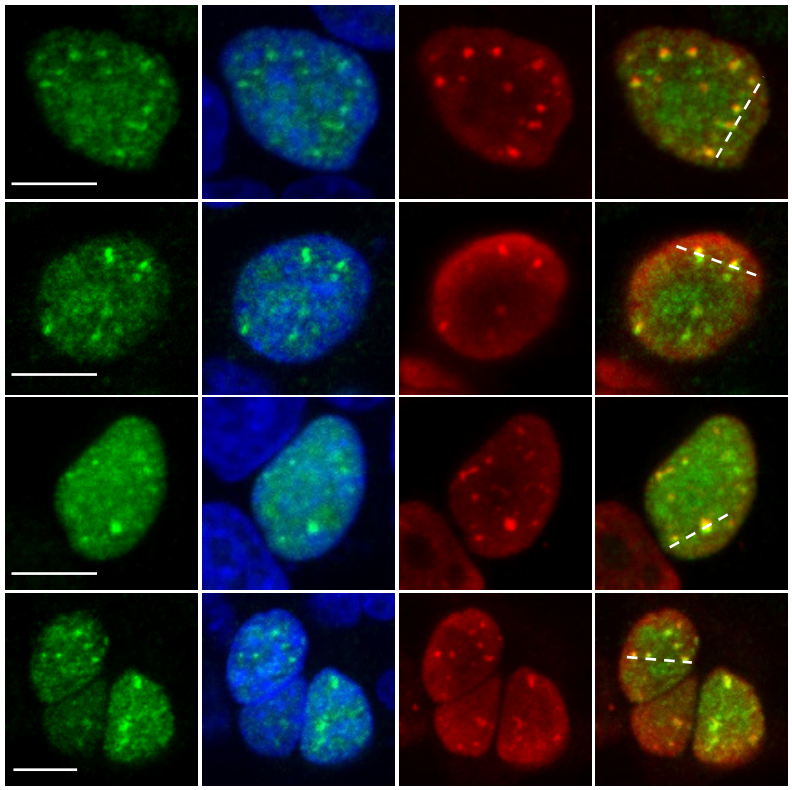

relative intensity

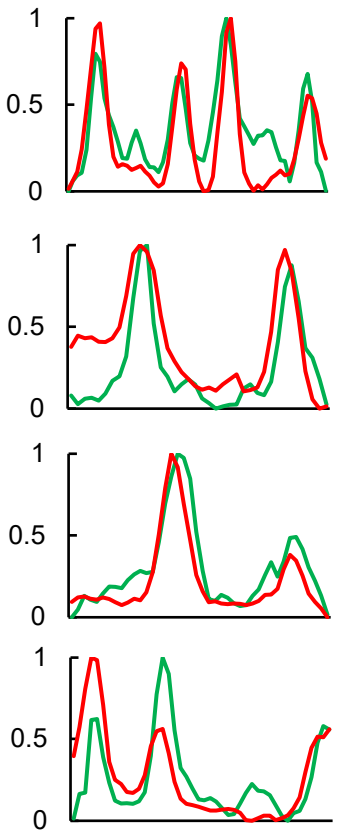

dCas13d-dsRBD + NT gRNA

HA-DAPI-hTR(3xFLAG-hTERT)

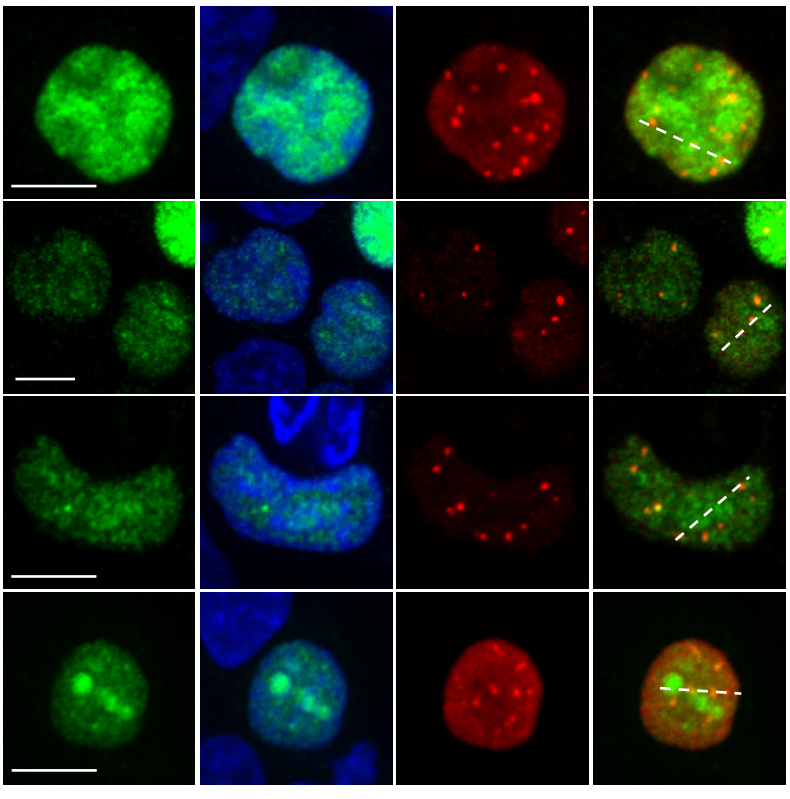

relative intensity

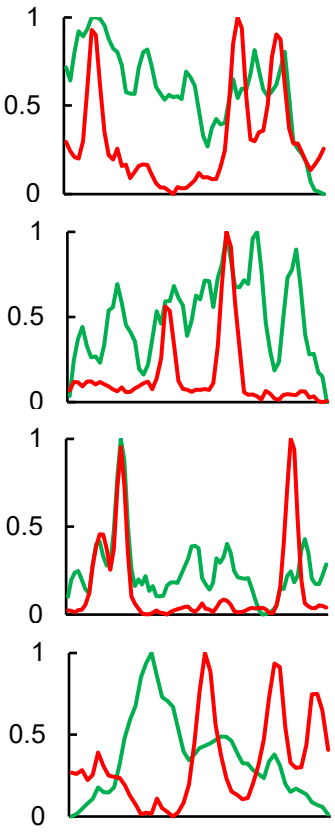

Figure S8. Fluorescence imaging of dCas13d-dsRBD localization. Same as in Figure 2B with additional fields of view.

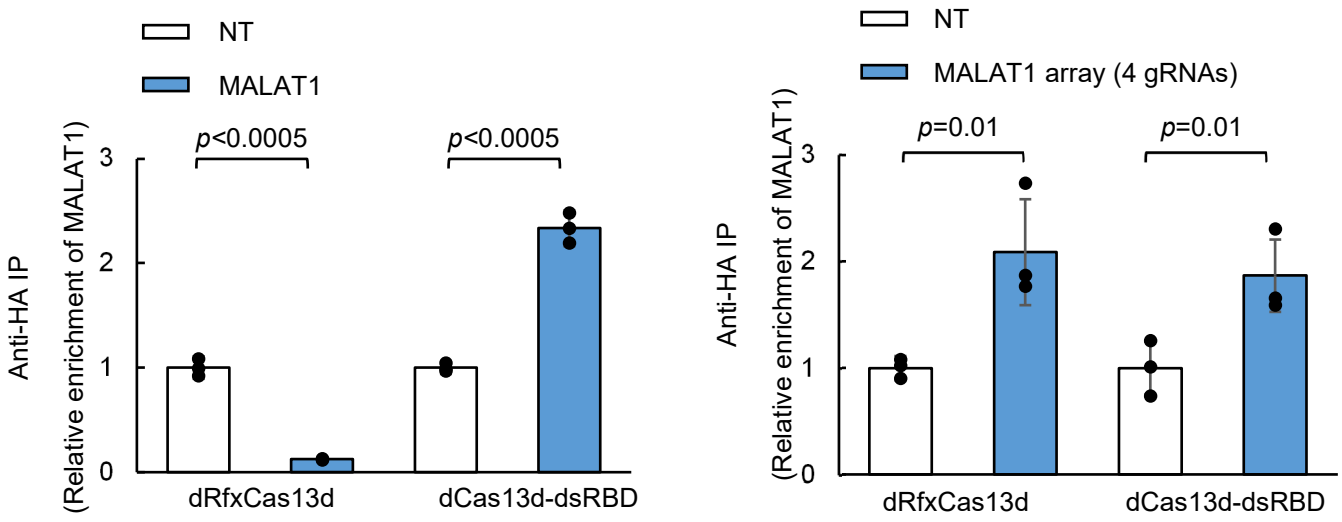

Figure S9. RNA immunoprecipitation experiment to show dCas13d-dsRBD binding to endogenous MALAT1 lncRNA. HEK293T cells are transfected with dRfxCas13d or dCas13d-dsRBD, together with a single MALAT1 gRNA (left) or a 4 MALAT1 gRNA array (right) (see Table S3 for sequences used). RNA bound to dCas13d is immunoprecipitated with anti-HA antibody followed by RT-qPCR quantitation. Data are analyzed using a one-tailed Student's t-test (n=3).

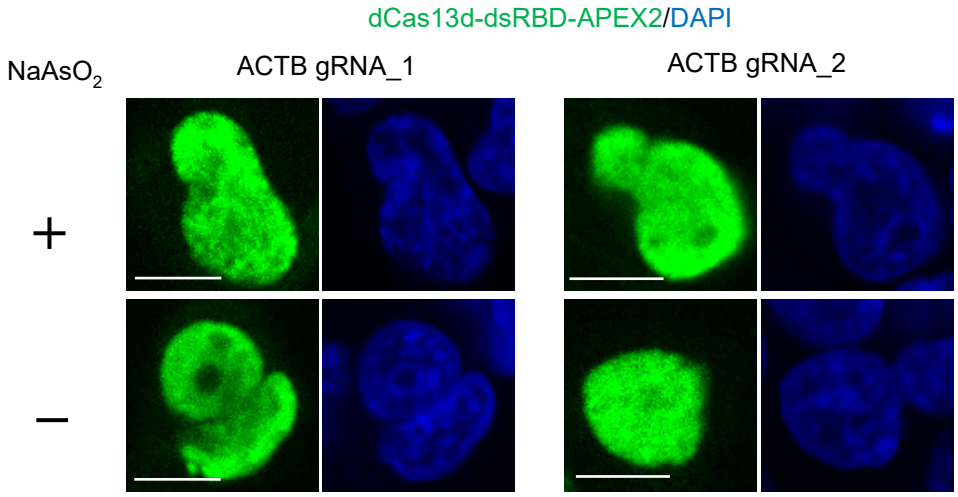

Figure S10. Testing dCas13d-dsRBD-APEX2 binding to endogenous ACTB mRNA during stress granule formation. HEK293T cells are co-transfected with dCas13d-dsRBD-APEX2 (Figure 2C) and gRNAs against ACTB mRNA for 48 hours, and then treated with $NaAsO_2$ for 30 minutes to induce stress granule formation. dCas13d is visualized by anti-V5 staining (Alexa Fluor 488, green). The nucleus is stained with DAPI. No cytosolic granules were observed with either ACTB gRNA by V5 staining. Scale bars, 10 μm.

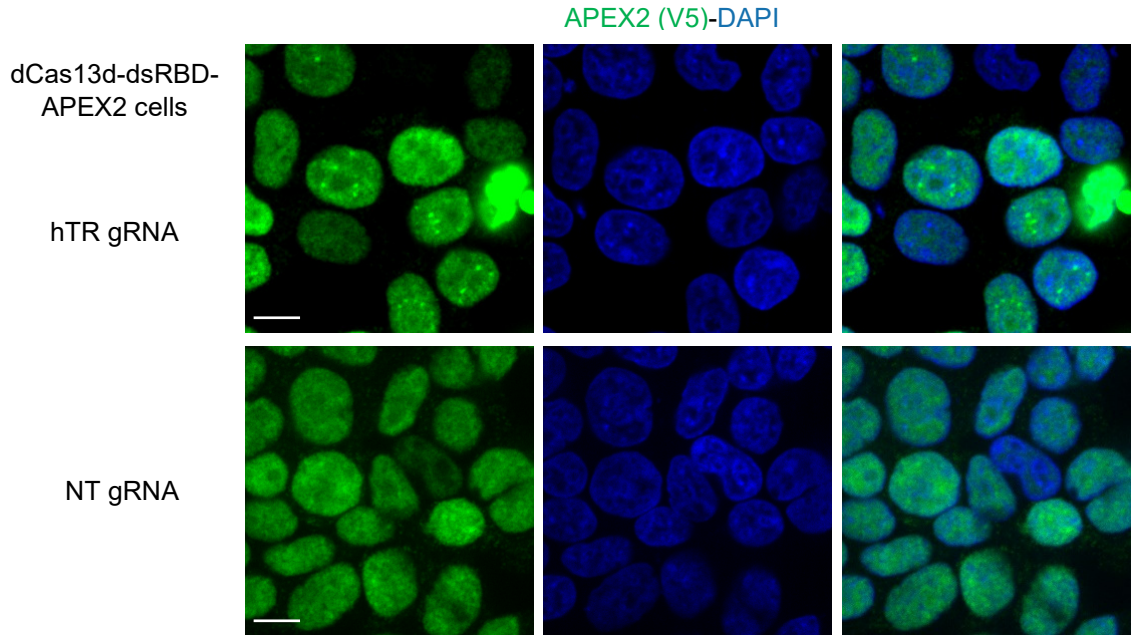

Figure S11. Fluorescence imaging of dCas13d-dsRBD-APEX2 localization. Clonal dCas13d-dsRBD-APEX2 (Figure 2C) HEK293T cells expressing untagged hTR along with either hTR gRNA or nontarget (NT) gRNA were fixed and stained with DAPI (nuclei) and anti-V5 antibody to visualize APEX2 (Alexa Fluor 647, green). Scale bars, 10 μm.

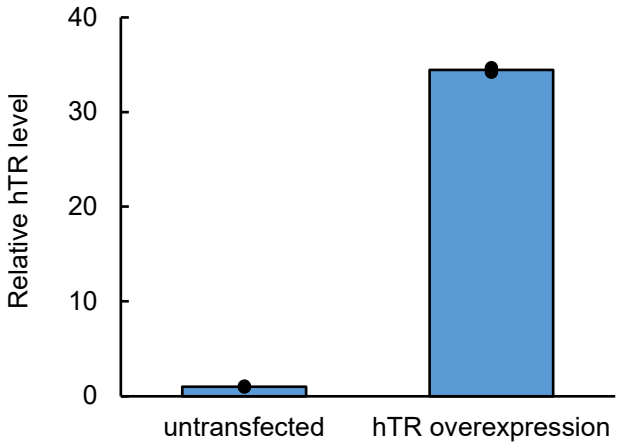

Figure S12. RT-qPCR of hTR expression level in untransfected and hTR-overexpressing cells. Total RNA extract from either sample was quantified by RT-qPCR. hTR expression level is normalized against untransfected cells. Data are from two biological replicates (n=2).

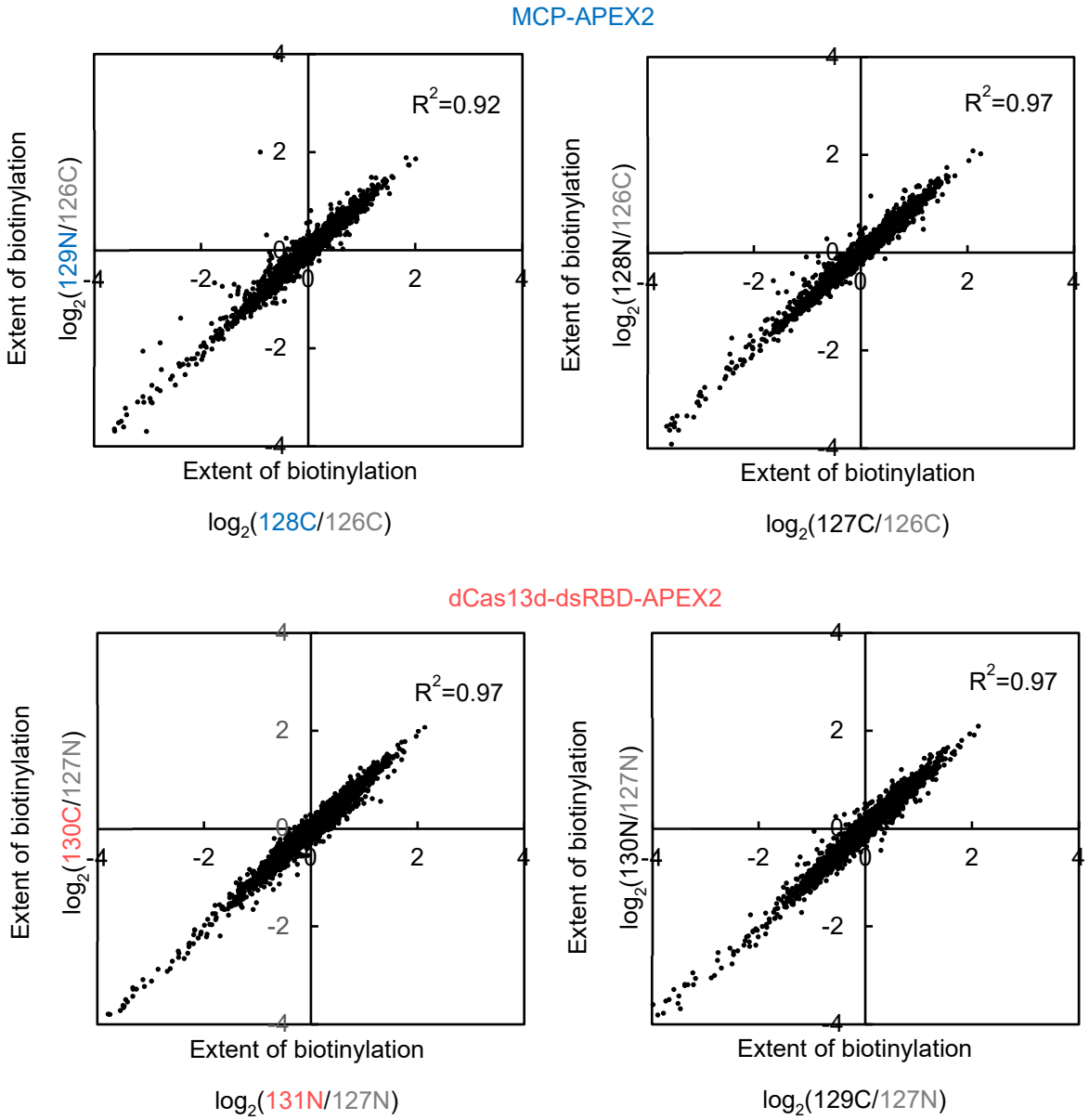

Figure S13. Scatter plots showing the correlation between replicates for both MCP-APEX2 samples and dCas13d-dsRBD-APEX2 samples. The extent of biotinylation by APEX2 for all detected proteins in replicate 1 is plotted against the same values from replicate 2.

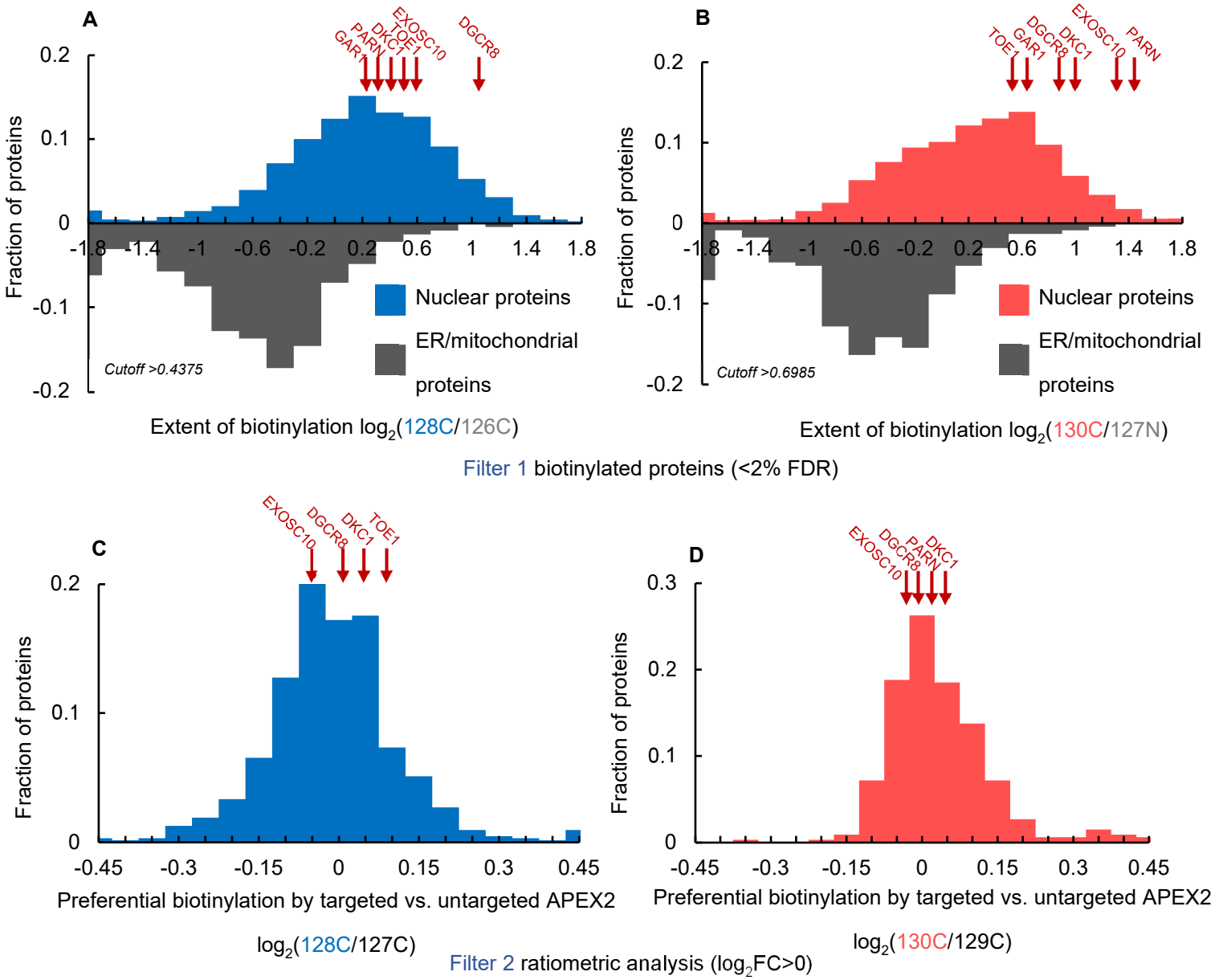

Figure S14. Histograms of proteomic data used to determine TMT ratio cutoffs. **(A, B)** Protein density histograms showing how Filter 1 cutoff was determined for (A) MCP-APEX2 samples and (B) dCas13d-dsRBD-APEX2 samples. True negatives (ER and mitochondrial proteins) are plotted in grey, and nuclear proteins are plotted in blue or red for MCP-APEX2 and dCas13d-dsRBD-APEX2 samples, respectively. Red arrows indicate the TMT ratios of known hTR binding proteins from Table S1. The cutoff was set at 2% false-discovery-rate (FDR) and each replicate was analyzed separately.
(C, D) Protein density histograms showing how Filter 2 cutoff was determined (after application of Filter 1) for (C) MCP-APEX2 samples and (D) dCas13d-dsRBD-APEX2 samples. Red arrows indicate the TMT ratios of known hTR binding proteins from Table S1. The cutoff was chosen based on preferential enrichment in the targeted APEX2 versus nontargeted APEX2 sample (log_2 fold change>0). Each replicate was analyzed separately.

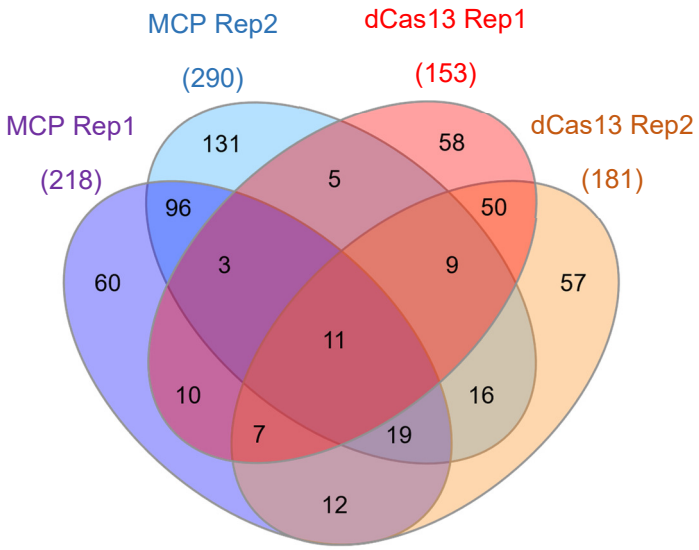

Figure S15. Venn diagram depicting the protein content overlap between proteomic datasets.

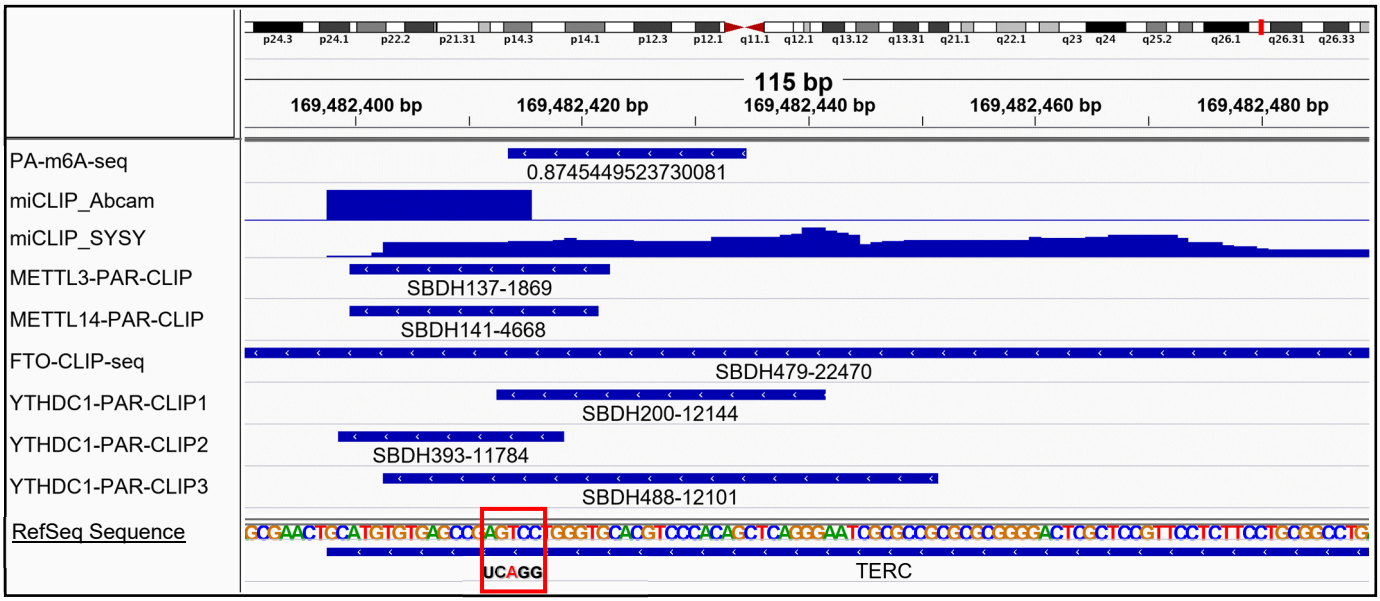

1. Chen et al, 2015, 1 of 4 repeats shows peak
2. Linder et al, 2015, 1 of 1 repeat shows peak
3. Linder et al, 2015, 1 of 1 repeat shows peak
4. Liu et al, 2014, 4 of 4 repeats show peak
5. Liu et al, 2014, 3 of 4 repeats show peak
6. Bartosovic et al, 2017, 3 of 3 repeats show peak
7. Xu et al, 2014, 1 of 2 repeats shows peak
8. Xiao et al, 2016, 1 of 2 repeats shows peak
9. Roundtree et al, 2017, 1 of 2 repeats shows peak

Figure S16. Genome tracks of published sequencing datasets (3–9) that support m^{6}A modification on hTR (TERC). The m^{6}A consensus motif GGACU is boxed in red with the putative methylated adenosine highlighted.

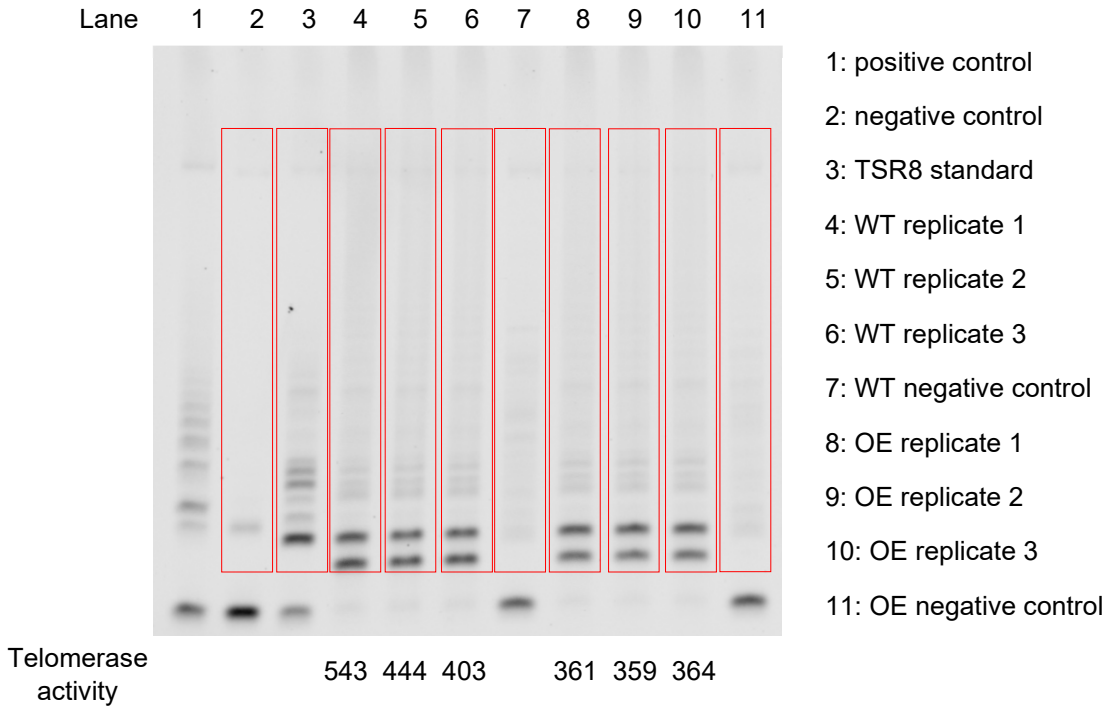

Figure S17. Telomerase activity assay. TBE (Tis-Borate-EDTA) gel showing PCR products from the PCR-based telomerase activity assay (TRAPeze kit). Positive control in lane 1 is the extract of telomerase positive cells from the kit; negative control in lane 2 is reaction buffer; TSR8 standard in lane 3 is an oligonucleotide primer that serves as a standard for quantitation; negative controls in lane 7 and 11 are heat-inactivated cell lysates. The intensity of each sample lane was quantified using ImageJ. The product region used for quantitation is boxed in red, which excludes the bottom internal control band. WT (lane 4-6) and OE samples (lane 8-10) were background corrected using negative control samples (lane 7 and 11, respectively). The telomerase activities of corrected samples were calculated using TSR8 standard according to the manufacturer's instruction and listed at the bottom of each sample lane.

gene ID	protein name	function (Pubmed ID)
TERT	Telomerase reverse transcriptase	telomerase component (21844345)
WRAP53	Telomerase Cajal body protein 1	telomerase component (21844345)
DKC1	H/ACA ribonucleoprotein complex subunit DKC1	telomerase component (21844345)
NHP2	H/ACA ribonucleoprotein complex subunit 2	telomerase component (21844345)
NOP10	H/ACA ribonucleoprotein complex subunit 3	telomerase component (21844345)
GAR1	H/ACA ribonucleoprotein complex subunit 1	telomerase component (21844345)
DGCR8	Microprocessor complex subunit DGCR8	hTR degradation (26687677)
EXOSC10	Exosome component 10	hTR degradation (26687677)
PARN	Poly(A)-specific ribonuclease PARN	hTR biogenesis (26482878)
TOE1	Target of EGR1 protein 1	hTR biogenesis (30371886)

Table S1. A literature-curated list of previously known hTR binding proteins. The table lists the function of each protein, with associated reference.

Plasmid Name	Promoter	Insert	Source
MCP-APEX2	CMV	NLS-V5-MCP-APEX2	This study
4xMS2-hTR	CMV	4xMS2 stem-loop-hTR-500 bp genomic sequence	This study
3xFLAG-hTERT	CMV	3xFLAG-hTERT	Addgene #51631
EGFP-coilin	CMV	3xFLAG-hTERT	Addgene #36906
EGFP-TCAB1	CMV	EGFP-TCAB1	Addgene #64676
dRfxCas13d	CMV	NLS-dRfxCas13d-NLS-HA	cloned from Addgene #109049
dCas13d-dsRBD	CMV	BPNLS-dRfxCas13d-dsRBD-BPNLS-HA	This study
dCas13d-dsRBD-APEX2	TetON	APEX2-V5-BPNLS-dRfxCas13d-dsRBD-BPNLS-P2A-GFP	This study
hTR	CMV	hTR-500 bp genomic sequence	This study
dRfxCas13d gRNAs	U6	Spacer sequences in Table S3	Vector from Addgene #109053
ALKBH5-FLAG	CMV	ALKBH5-FLAG	Lichinchi et al, *Cell Host Microbe* 2016
dPspCas13b	CMV	NLS-dPspCas13b-3xEGFP-NLS-3xFLAG	Addgene #132398
ATP5B-3'UTR-2xMS2	CMV	ATP5B-3'UTR-2xMS2 stem-loop	Ortega *et al*, *J. Cell Sci.* 2010
ACTB-3'UTR-2xMS2	CMV	ACTB-3'UTR-2xMS2 stem-loop	Cloned from Addgene #27123
G3BP1-GFP	CMV	G3BP1-GFP	Aulas *et al*, *J. Cell Biol.* 2015

Table S2. A list summarizing the plasmid constructs used in this study.

Name	Sequence (5'-3')
qPCR_hTR_Forward primer	TCTAACCCTAACTGAGAAGGGCGTAG
qPCR_hTR_Reverse primer	GTTTGCTCTAGAATGAACGGTGGAAG
qPCR_MALAT1_Forward primer	GAATTGCGTCATTTAAAGCCTAGT
qPCR_MALAT1_Reverse primer	CCGTACTTCTGTCTTCCAGTTT
qPCR_HOTAIR_Forward primer	CCAGAGAACGCTGGAAAAACCTG
qPCR_HOTAIR_Reverse primer	GGAGATGATAAGAAGAGCAAGGAA
qPCR_GAPDH_Forward primer	TTCGACAGTCAGCCGCATCTTCTT
qPCR_GAPDH_Reverse primer	GCCCAATACGACCAAATCCGTTGA
RfxCas13d_Spacer_nontarget	TCACCAGAAGCGTACCATACTC
RfxCas13d_Spacer_hTR_gRNA1	CTCCCAGGCCCACCCTCCGCAA
RfxCas13d_Spacer_hTR_gRNA2	CGCCTACGCCCTTCTCAGTTAG
RfxCas13d_Spacer_hTR_gRNA3	GGGAGCAAAAGCACGGCGCCTA
RfxCas13d_Spacer_hTR_gRNA4	CCCGCTGAAAGTCAGCGAGAAA
RfxCas13d_Spacer_hTR_gRNA5	TTTGCTCTAGAATGAACGGTGG
RfxCas13d_Spacer_hTR_gRNA6	TGTGAGCCGAGTCCTGGGTGCA
RfxCas13d_Spacer_MALAT1	TAACCAACTTCCCCTTCTAGCT
RfxCas13d_Spacer array_MALAT1_1	GTATTTATAGACGGAGAACAACTCGCATCA
RfxCas13d_Spacer array_MALAT1_2	CTTCTCCAAATTGTTTCATCCTACCACTCC
RfxCas13d_Spacer array_MALAT1_3	CTATCTTCTATACTTCTCCAATACTTGTCT
RfxCas13d_Spacer array_MALAT1_4	TAACCAACTTCCCCTTCTAGCTTCAAGTAT
RfxCas13d_Spacer_ACTB_gRNA1	CTGGCGGCGGGTGTGGACGGGC
RfxCas13d_Spacer_ACTB_gRNA2	GAGCCACACGCAGCTCATTGTA

Table S3. A list summarizing 1) the RT-qPCR primers in this study; 2) the spacer sequence of the RfxCas13d guide RNAs used in this study.

Dataset S1. Proteomic data and analysis. Tab 1: all proteomic data after removing non-human contaminants and 2 unique peptide cutoff; Tab 2: final proteome of 129 proteins from MCP-APEX2 experiment; Tab 3: final proteome of 77 proteins from dCas13d-dsRBD-APEX2 experiment; Tab 4: 49 proteins enriched in ≥3 datasets. Tab 5: 11 proteins enriched in all 4 datasets. Tab 6: hTR specificity of proteins enriched in more than 3 datasets and all 4 datasets; Tab 7: column definitions of the spreadsheet.

SI Appendix Methods

Plasmid construction

The MCP-APEX2 construct (NLS-V5-MCP-APEX2) was created by cloning into the lentiviral vector pLX304 using Gibson assembly. The dCas13d-dsRBD-APEX2 construct (dox inducible APEX2-V5-BPNLS-dRfxCas13d-dsRBD-BPNLS-P2A-GFP) was created by cloning into an all in one piggybac, TREG/Tet-3G plasmid via Gibson assembly. The sequence of bipartite SV40NLS (BPNLS) is selected as previously described (10). The dsRBD is taken from the double-stranded RNA binding motif (amino acid 2-81) in the protein EIF2AK2. The hTR expression plasmids were constructed by putting either MS2 stem-loop tagged or native hTR sequences under the CMV promoter, followed by 500 bp genomic sequence flanking the 3' of hTR. Guide RNA sequences were selected and cloned into a human U6 promoter containing vector as previously described (11). Spacer sequences of the gRNAs are listed in Table S3. The ALKBH5-FLAG construct was cloned into the pcDNA3 vector. The following constructs were obtained from Addgene: FLAG-hTERT (#51631), EGFP-coilin (#36906), EGFP-TCAB1 (#64676), RfxCas13d (#109049), dRfxCas13d (#109050). The plasmid constructs and their features are listed in Table S2.

Gels and western blots

Clarified lysates were boiled for 10 minutes at 95ºC before loading onto an SDS-PAGE gel (Invitrogen). Gels were transferred to nitrocellulose membrane, stained by Ponceau S (10 minutes in 0.1% [w/v] Ponceau S in 5% acetic acid/water). The blots were then blocked 3% BSA in TBS-T (Tris-buffered saline, 0.1% Tween 20) at room temperature for 1 hour and stained with 0.3 µg/mL streptavidin-HRP (BioRad) in TBS-T for 1 hour at room temperature. The blots were washed four times with TBS-T for 5 min each prior to developing with Clarity Western ECL Blotting Substrates (BioRad) and imaging on a UVP BioSpectrum Imaging System. Silver-stained gels of enriched material eluted from the streptavidin beads were generated using Pierce Silver Stain Kit (Thermo).

On-bead digestion and liquid chromatography mass spectrometry

Mass spectrometry-based proteomic experiment was performed as previously described with minor modifications (12). Briefly, after enrichment and washing, beads were resuspended in 50 mM TRIS pH 8, 150 mM NaCl, and frozen until digestion. After thawing, dry urea was added to the solution to 8M, along with TCEP and iodoacetamide to 5 mM, followed by incubation for 30 minutes at 25ºC. The beads were diluted to 4 M urea with resuspension buffer above, and 1 uL of LysC (Wako) was added and incubated at 37ºC for two hours. The urea was again diluted to 2 M and 800 ng trypsin was added for overnight digestion at 37ºC. The following day the digests were acidified, desalted, TMT (tandem mass tag)-labeled on-column, and fractionated according to previous reports(12), with the exception that 100 mM potassium phosphate pH 8.0 was used in place of HEPES during the on-column TMT labeling. Six basic reverse-phased fractions were generated, concatenated to three and analyzed using an EASY-nLC 1200 coupled to a Q-Exactive Plus mass spectrometer (Thermo).

Immunofluorescence staining

HEK 293T cells were plated onto glass coverslips in 48-wells 18-24 hours prior to transfection using lipofectamine 2000. The following amount of each plasmid was used: 50-70 ng of the MCP-APEX2 plasmid, 50-70 ng of the FLAG-hTERT plasmid, 50-70 ng of the EGFP-TCAB1 plasmid, 50-70 ng of the dRfxCas13d plasmid, 50-70 ng of the dCas13d-dsRBD plasmid, 400-500 ng of the 4×MS2-hTR plasmid, 400-500 ng of the hTR plasmid, 400-500 ng of the gRNA plasmid, 300 ng of the ALKBH5-FLAG plasmid. 24 hours after transfection, the cells were fixed with 4% (v/v) paraformaldehyde in PBS buffer at room temperature for 15 minutes. Cells were then washed three times with PBS and permeabilized with cold methanol at −20°C for 5-10 min. Cells were then washed three times with PBS, and then incubated with primary antibody in PBS supplemented with 3% (w/v) BSA for 1 hour at room temperature. After washing three times with PBS, cells were then incubated with DAPI and secondary antibody in PBS supplemented with 3% (w/v) BSA for 30 minutes at room temperature. Cells were then washed three times with PBS and imaged by confocal fluorescence microscopy. The following primary and secondary antibodies were used: mouse anti-V5 (Life Technologies, 1:1000 dilution), mouse anti-FLAG (Agilent, 1:800 dilution), rabbit anti-V5 (GenScript, 1:500 dilution), rabbit anti-HA (Cell Signaling, 1:1000 dilution), FLAG-PE (Miltenyi

Biotec, 1:500 dilution), rabbit anti-TCAB1 (Bethyl Laboratories, 1:500 dilution), mouse anti-DKC1 (Santa Cruz Biotech, 1:500 dilution), goat anti-mouse Alexa Fluor405 (Invitrogen, 1:1000 dilution), goat anti-mouse Alexa Fluor488 (Invitrogen, 1:1000 dilution), goat anti-mouse Alexa Fluor647 (Invitrogen, 1:1000 dilution), goat anti-rabbit Alexa Fluor405 (Invitrogen, 1:1000 dilution), goat anti-rabbit Alexa Fluor488 (Invitrogen, 1:1000 dilution), and goat anti-rabbit Alexa Fluor647 (Invitrogen, 1:1000 dilution).

Confocal fluorescence imaging

Confocal imaging was performed using a Zeiss AxioObserver.Z1 microscope, outfitted with a Yokogawa spinning disk confocal head, a Cascade II:512 camera, a Quad-band notch dichroic mirror (405/488/568/647), 405 (diode), 491 (DPSS), 561 (DPSS), and 640 (diode) nm lasers (all 50 mW). DAPI (405 laser excitation, 445/40 emission), Alexa Fluor568 (561 laser excitation, 617/73 emission), phycoerythrin (561 laser excitation, 617/73 emission), and Alexa Fluor647 (640 laser excitation, 700/75 emission), and differential interference contrast (DIC) images were acquired through a 63× oil-immersive objective. All images were collected, processed, and analyzed using the SlideBook 6.0 software (Intelligent Imaging Innovations).

m^{6}A pulldown assay

HEK293T cells are plated in 10-cm dishes at 70-80% confluency. 18 hours after plating, cells were either directly harvested or transfected with 20 μg of the ALKBH5 plasmid with lipofectamine and then harvested 48 hours post transfection. To harvest the cells, each 10-cm dish of cells were lifted, washed with PBS for two times, and collected by centrifuge. 5mL Trizol (Thermo) was used to homogenize the cell pellets and total RNA was extracted according to manufacturer's protocol by precipitation. m^{6}A pulldown was performed with a rabbit monoclonal anti-m^{6}A antibody in the EpiMark *N*^{6}-Methyladenosine Enrichment Kit (NEB) according to the manufacturer's protocol. Briefly, 80 μg of total RNA was subject to m^{6}A enrichment by incubating with 25 μL Protein G magnetic beads (Pierce) coupled with 2 μL m^{6}A antibody at 4 °C for 1 hour with rotation, washed 6 times, and eluted with Buffer RLT (Qiagen). Two control samples were processed in parallel: one control used 10 μL m^{6}A-modified RNA (100 nM) supplied in the kit for pre-incubation with the m^{6}A antibody at 4 °C for 30 minutes to block the antibody; the other used 2 μL rabbit monoclonal anti-HA antibody (Cell Signaling) as a control IgG for pulldown. The eluate was further purified and concentrated with RNA Clean and Concentrator kit (Zymo). Target genes in input total RNA and enriched RNA were quantified by qRT-PCR using SuperScript III Platinum One-Step qRT-PCR Kit (Invitrogen).

Telomerase activity assay

HEK293T cells are plated in 10-cm dishes at 70-80% confluency. 18 hours after plating, cells were transfected with 20 μg of the ALKBH5 plasmid with lipofectamine and then harvested 48 hours post transfection with ~30-40% transfection efficiency. Telomerase activity is measured with the TRAPeze Telomerase Detection Kit (Millipore) according to manufacturer's protocol. Briefly, HEK cells were lifted from plates and washed twice with PBS, resuspended to single cells, counted using Countess II FL Automated Cell Counter (Thermo) and aliquoted in exactly 1 million cells per tube and collected by centrifugation. The cell pellets were flash frozen with liquid nitrogen and stored at -80 °C until ready for use. The cell pellets were later lysed using 200 μL of 1×CHAPS lysis buffer supplied with the kit on ice for 30 minutes, centrifuged, and the supernatant was collected and aliquoted for storage in -80 °C. Each aliquot was used only once. For the telomerase activity assay, each reaction was set up in half scale (25 μL/reaction with 1 μL of lysate) according to the kit protocol, subjected to 32 cycles of PCR, and run on 10% TBE gel in 0.5x TBE buffer for 1 hour at 160V. The gel was then stained in 100 mL water with 10,000x SybrSafe (Thermo) stain at room temperature for 30 minutes, washed with water for 20 minutes, and imaged on a ChemiDoc MP Imaging System (Bio-rad). The DNA products were quantified with ImageJ by signal integration of the product region (boxed in red in Fig. S17) and background correction with heat-inactivated samples. TPG (Total Product Generated) units were calculated using the signal of TSR8 standard lane corrected with negative control lane according to the instructions in the kit.

References in SI Appendix

1. J. L. Chen, M. A. Blasco, C. W. Greider, Secondary structure of vertebrate telomerase RNA. *Cell* **100**, 503–14 (2000).
2. L. Z. Yang, *et al.*, Dynamic Imaging of RNA in Living Cells by CRISPR-Cas13 Systems. *Mol. Cell* **76**, 981-997.e7 (2019).
3. K. Chen, *et al.*, High-resolution N6-methyladenosine (m6A) map using photo-crosslinking-assisted m6A sequencing. *Angew. Chemie - Int. Ed.* **54**, 1587–1590 (2015).
4. B. Linder, *et al.*, Single-nucleotide-resolution mapping of m6A and m6Am throughout the transcriptome. *Nat. Methods* **12**, 767–772 (2015).
5. J. Liu, *et al.*, A METTL3-METTL14 complex mediates mammalian nuclear RNA N6-adenosine methylation. *Nat. Chem. Biol.* **10**, 93–95 (2014).
6. M. Bartosovic, *et al.*, N6-methyladenosine demethylase FTO targets pre-mRNAs and regulates alternative splicing and 3′-end processing. *Nucleic Acids Res.* **45**, 11356–11370 (2017).
7. C. Xu, *et al.*, Structural basis for selective binding of m6A RNA by the YTHDC1 YTH domain. *Nat. Chem. Biol.* **10**, 927–929 (2014).
8. W. Xiao, *et al.*, Nuclear m6A Reader YTHDC1 Regulates mRNA Splicing. *Mol. Cell* **61**, 507–519 (2016).
9. I. A. Roundtree, *et al.*, YTHDC1 mediates nuclear export of N6-methyladenosine methylated mRNAs. *Elife* **6** (2017).
10. J. Wu, A. H. Corbett, K. M. Berland, The intracellular mobility of nuclear import receptors and NLS cargoes. *Biophys. J.* **96**, 3840–3849 (2009).
11. S. Konermann, *et al.*, Transcriptome Engineering with RNA-Targeting Type VI-D CRISPR Effectors. *Cell* **173**, 665-676.e14 (2018).
12. S. A. Myers, *et al.*, Discovery of proteins associated with a predefined genomic locus via dCas9–APEX-mediated proximity labeling. *Nat. Methods* **15**, 437–439 (2018).